[12] W. J. R. Hoefer, "Fin-line design made easy," in *1978 IEEE MTT-S Int. Microwave Symp. Dig.*, (Ottawa, Canada), p. 471.
[13] A. K. Sharma and W. J. R. Hoefer, "Empirical expressions for finline design," *IEEE Trans. Microwave Theory Tech.*, vol. MTT-31, pp. 350–356, Apr. 1983.
[14] A. M. K. Saad and K. Schunemann, "A simple method for analysing fin-line structures," *IEEE Trans. Microwave Theory Tech.*, vol. MTT-26, Dec. 1978.
[15] M. N. Burton and W. J. R. Hoefer, "Closed-form expressions for the parameters of finned and ridged waveguides," *IEEE Trans. Microwave Theory Tech.*, vol. MTT-30, pp. 2190–2194, Dec. 1982.
[16] R. F. Harrington, *Time Harmonic Electromagnetic Fields*. New York: McGraw-Hill, 1961, p. 345.
[17] H. Meinel and B. Rembold, "New millimeter wave fin-line attenuators and switches," in *1979 IEEE MTT-S Int. Microwave Symp. Dig.*, (Orlando, FL), pp. 249–252.
[18] P. Pramanick and P. Bhartia, "Analysis and synthesis of tapered fin-lines," presented at IEEE MTT-S, Int. Symp., San Francisco, CA, 1984.

Protap Pramanick obtained the B.Tech. (Hons.) degree in electronics and communication engineering from the Indian Institute of Technology in 1977 and the Ph.D. degree in electrical engineering from the Indian Institute of Technology, Kanpur, in 1982.

From 1978 to 1980, he was a Research Assistant in the Department of Electrical Engineering, Indian Institute of Technology, Kanpur, and from 1980 to 1982, he was a Senior Research Assistant in the same department. In September 1982, he joined the Department of Electrical Engineering, the University of Ottawa, Canada, as a Research Associate. Since November 1984, he has been with the Canadian Marconi Company, Ottawa, as a member of the research staff. His main fields of interest include microwave measurements, and microwave and millimeter-wave integrated circuits. Dr. Pramanick has authored or co-authored over 30 technical papers.

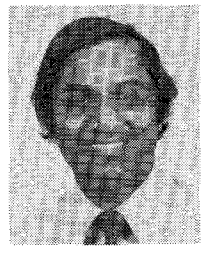

Prakash Bhartia (S'68–M'71–SM'76) obtained the B.Tech. (Hons.) degree in electrical engineering from the Indian Institute of Technology, Bombay, in 1966, and the M.Sc and Ph.D degrees from the University of Manitoba, Winnipeg, Canada, in 1968 and 1971, respectively.

From 1971 to 1973, he was a Research Associate at the University of Manitoba and joined the Faculty of Engineering at the University of Regina in 1973, where he served as Assistant Dean. In 1977, he joined the Defense Research Establishment, Ottawa, and was simultaneously appointed an Adjunct Professor at the University of Ottawa. He has conducted research in both theoretical and applied electromagnetics, scattering, diffraction, radio, satellite, and inertial navigation, etc. He is currently Head of Electromagnetics at DREO with responsibility for programs in Navigation, Electromagnetic Compatibility, and Electromagnetic Pulse Effects. He has authored or co-authored over 100 technical papers, two books, *Microstrip Antennas* (Artech House) and *Millimeter Wave Engineering and Applications* (J. Wiley & Sons), and holds a number of patents.

Dr. Bhartia is a Fellow of the Institution of Electronics and Telecommunication Engineers, an Associate Editor of the *Journal of Microwave Power*, and serves on the Editorial Review Boards of MTT and AP.

General Stability Analysis of Periodic Steady-State Regimes in Nonlinear Microwave Circuits

VITTORIO RIZZOLI, MEMBER, IEEE, AND ALESSANDRO LIPPARINI

Abstract — **The problem of analyzing the stability of periodic equilibrium regimes in nonlinear microwave circuits is tackled by a general-purpose computer-aided approach. By means of a perturbation technique, the search for instabilities is reduced to a generalized eigenvalue equation expressed in matrix form, and is then carried out by Nyquist's analysis. The use of a vector processor allows the computer time requirements to be kept well within reasonable limits, even in the case of large-size problems. In perspective, this could open the way to the complementation of existing nonlinear CAD packages by an on-line facility for automatic stability analysis.**

Manuscript received April 24, 1984; revised August 2, 1984. This work was supported in part by the Italian Ministry of Public Education.

The authors are with Dipartimento di Elettronica, Informatica e Sistemistica, University of Bologna, Villa Griffone, 40044 Pontecchio Marconi, Bologna, Italy.

I. Introduction

THIS PAPER is devoted to introducing a new numerical technique for analyzing the stability of periodic steady-state regimes in nonlinear microwave circuits. This problem is a very difficult one, and has been tackled in the literature by a variety of approximations and limiting assumptions (e.g., [1]–[6]). From time to time, the analysis has been restricted to specific kinds of nonlinear devices, and/or the representation of the perturbed regime has been severely simplified, either by reducing the number of spectral lines to be accounted for, or by resorting to the concept of slowly changing perturbation.

On the other hand, the emphasis here is on generality. At least in principle, our all-computer approach should be

0018-9480/85/0100-0030$01.00 ©1984 IEEE

able to cope with almost any kind of realistic nonlinear device models, and with the complex circuit topologies encountered in practical microwave engineering applications. To do so, no restrictions are imposed on the time-domain representation of the nonlinear devices. Furthermore, within the frame of a perturbation technique, we take into account all the spectral lines arising from the interaction of a perturbing signal with the nonsinusoidal steady-state regime in the nonlinear part of the network. As a result, the program can be used to search for instabilities in a wide variety of nonlinear subsystems, such as amplifiers, oscillators, and parametric circuits, with minimum effort on the user's side.

In exchange for these attractive features, the method is purely numerical in nature, and makes no allowance for physical intuition. Furthermore, in some cases, it is very demanding in terms of computer time, since repetitive calculations on large-order matrices may be required. Thus, to ensure a good cost-effectiveness in the generality of applications, the present approach is best implemented on a "supercomputer" (Cyber 205 or similar); in fact, the formulation adopted lends itself nicely to the development of a highly vectorized code, allowing the hardware capabilities of a vector processor to be fully exploited.

It is quite obvious that the validity of a numerical technique cannot be demonstrated, but only checked, since results are only available for particular cases. In this paper, we present two different checks, as an attempt to enhance the reader's confidence in our approach.

The first one is essentially mathematical and concerns the simple case of a monochromatic free-running oscillator subject to slowly changing perturbations. This problem can be solved in closed form, and the explicit stability conditions given by Hansson and Lundsrtöm [5] and Kurokawa [6] are reobtained as particular cases of the general equations. Thus, it is the inherent difficulty of the general stability problem that warrants the mathematical complexity of our method: simple situations generate simple solutions which agree with classic ones.

The second check is a large-size numerical application concerning a real-world circuit, and is chosen in such a way that the results of the stability analysis can easily be predicted on a qualitative ground by physical intuition. In fact, we find that the hysteresis cycle appearing in the power transfer characteristic of a microstrip frequency divider is associated with the existence of unstable steady-state regimes.

II. Description of the Method

We consider the nonlinear network schematically depicted in Fig. 1, with $\mathcal{N}_L$ representing an arbitrary linear multiport, and $\mathcal{N}$ the nonlinear part of the circuit, usually a set of semiconductor devices. The currents and voltages at the ports of $\mathcal{N}$ are used as the state variables. For the sake of simplicity, in the following we will make the assumption that both $\mathcal{N}$ and $\mathcal{N}_L$ are one-ports—the extension to the general case is straightforward and only

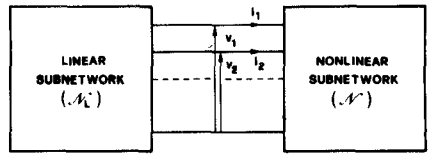

Fig. 1. Schematic representation of general nonlinear network.

requires scalar quantities (such as currents or admittances) to be replaced by their vector counterparts.

The nonlinear subnetwork $\mathcal{N}$ is described by the time-domain equation

$$f[F^{-l}i,\cdots,F^{n}i;\ F^{-l}v,\cdots,F^{n}v]=0 \tag{1}$$

where f is nonlinear and analytically known, but otherwise arbitrary. For the sake of brevity, the following operators have been introduced in (1):

$$\begin{aligned} F^{m}a &\equiv \frac{d^{m}}{dt^{m}}a(t)(m>0)\\ F^{0}a &\equiv a(t)\\ F^{-m}a &\equiv \int_{-\infty}^{t} du_1 \int_{-\infty}^{u_1} du_2 \cdots \int_{-\infty}^{u_{m-1}} du_m\, a(u_m)(m>0) \end{aligned} \tag{2}$$

where $a(t)$ is any function of time.

The linear subnetwork $\mathcal{N}_L$ is represented at any angular frequency ω by the usual frequency-domain equation (Fig. 1)

$$I=-Y(\omega)V+J(\omega) \tag{3}$$

where I, V are current and voltage phasors, $Y(\omega)$ is the admittance, and $J(\omega)$ is the Norton equivalent current source of any free generator acting within $\mathcal{N}_L$ at frequency ω (e.g., the pump of a parametric divider).

We now assume that the circuit can support a time-periodic steady-state electrical regime with a fundamental angular frequency ω_0. The state variables will thus have the expressions

$$\begin{aligned} \tilde{i}(t) &= \mathrm{Re}\left[\sum_{k=0}^{\infty} \tilde{I}_k \exp(jk\omega_0 t)\right]\\ \tilde{v}(t) &= \mathrm{Re}\left[\sum_{k=0}^{\infty} \tilde{V}_k \exp(jk\omega_0 t)\right] \end{aligned} \tag{4}$$

where $\sim$ denotes steady-state quantities. $\tilde{i}(t), \tilde{v}(t)$ satisfy the nonlinear equation (1), while their kth harmonics $\tilde{I}_k, \tilde{V}_k$ are related by (3) at $\omega = k\omega_0$. For a given circuit topology, $\tilde{I}_k$ and $\tilde{V}_k$ may easily be obtained by a circuit analysis based on the harmonic-balance technique [7].

If the equilibrium condition is perturbed by injection of a *small* signal of the form

$$\exp\{(\sigma+j\omega)t\} \tag{5}$$

where ω is not an integer multiple of ω_0 and $\sigma>0$, all possible intermodulation products of ω and ω_0 will be generated. However, since the perturbing signal is small, higher order terms in ω may be neglected, so that the

resulting perturbation takes the form

$$\Delta i(t) = \exp(\sigma t)\cdot \mathrm{Re}\left[\sum_{k=-\infty}^{\infty} \Delta I_k \exp\{j(\omega + k\omega_0)t\}\right]$$
$$\Delta v(t) = \exp(\sigma t)\cdot \mathrm{Re}\left[\sum_{k=-\infty}^{\infty} \Delta V_k \exp\{j(\omega + k\omega_0)t\}\right] \quad (6)$$

where ΔI_k, ΔV_k are *a priori* undetermined complex amplitudes.

Now, let us consider the perturbed regime

$$i(t) = \tilde{i}(t) + \Delta i(t)$$
$$v(t) = \tilde{v}(t) + \Delta v(t) \quad (7)$$

which must satisfy the network equations (1) and (3). From (3) we get

$$\Delta I_k = -Y(\omega - j\sigma + k\omega_0)\,\Delta V_k \quad (8)$$

so that only the ΔV_k's (say) are independent unknowns. On the other hand, replacing (7) into (1) under the assumption of a small perturbation yields

$$\sum_{m=-l}^{n} \left[\left.\frac{\partial f}{\partial x_m}\right|_{\sim} \cdot F^m \Delta i + \left.\frac{\partial f}{\partial y_m}\right|_{\sim} \cdot F^m \Delta v\right] = 0 \quad (9)$$

where the partial derivatives are evaluated in steady-state conditions ($\sim$) and

$$x_m = F^m i, \qquad y_m = F^m v, \qquad -l \leqq m \leqq n. \quad (10)$$

The operators F^m appearing in (9) and (10) are the same as defined by (2).

Since the steady-state regime is periodic, we can introduce the Fourier expansions

$$\left.\frac{\partial f}{\partial x_m}\right|_{\sim} = \sum_{p=-\infty}^{\infty} C_{mp} \exp(jp\omega_0 t)$$
$$\left.\frac{\partial f}{\partial y_m}\right|_{\sim} = \sum_{p=-\infty}^{\infty} D_{mp} \exp(jp\omega_0 t). \quad (11)$$

Because f is analytically known, so are its derivatives; making use of (4), the coefficients C_{mp}, D_{mP} may then be computed by the Fast Fourier Transform in a straightforward way. From (6) and (8), we further obtain $(-l \leqq m \leqq n)$

$$F^m \Delta i = -\exp(\sigma t) \cdot \mathrm{Re}\left[\sum_{k=-\infty}^{\infty} \{\sigma + j(\omega + k\omega_0)\}^m Y(\omega - j\sigma + k\omega_0) \cdot \Delta V_k \exp\{j(\omega + k\omega_0)t\}\right]$$

$$F^m \Delta v = \exp(\sigma t) \cdot \mathrm{Re}\left[\sum_{k=-\infty}^{\infty} \{\sigma + j(\omega + k\omega_0)\}^m \cdot \Delta V_k \exp\{j(\omega + k\omega_0)t\}\right]. \quad (12)$$

Now we make use of (11) and (12) to rewrite (9) in the form

$$\mathrm{Re}\left[\exp(j\omega t)\cdot \sum_{p=-\infty}^{\infty} \sum_{k=-\infty}^{\infty} \cdot \exp\{j(p+k)\omega_0 t\} A_{k,p} \Delta V_k\right] = 0 \quad (13)$$

where

$$A_{k,p} = \sum_{m=-l}^{n} \{\sigma + j(\omega + k\omega_0)\}^m D_{mp} - Y(\omega - j\sigma + k\omega_0) \cdot \sum_{m=-l}^{n} \{\sigma + j(\omega + k\omega_0)\}^m C_{mp}. \quad (14)$$

Finally, the double summation in (13) is rearranged by letting $s = p + k$ and using s and k as the new summation indexes. Equation (13) is thus turned into

$$\mathrm{Re}\left[\sum_{s=-\infty}^{\infty} \exp\{j(\omega + s\omega_0)t\} \cdot \sum_{k=-\infty}^{\infty} A_{k,s-k} \Delta V_k\right] = 0. \quad (15)$$

The left-hand side of (15) is a continuous function of time having a discrete frequency spectrum. In order to make it identically equal to zero, we must impose that all the spectral lines separately vanish, that is,

$$\begin{cases} \sum_{k=-\infty}^{\infty} A_{k,s-k} \Delta V_k = 0 \\ -\infty < s < \infty. \end{cases} \quad (16)$$

Equation (16) is a linear homogeneous system for the unknowns ΔV_k. If we denote by $\Delta(\sigma + j\omega)$ its determinant, then the possible unstable perturbations can be found by solving the generalized eigenvalue problem

$$\Delta(\sigma + j\omega) = 0. \quad (17)$$

When no eigenvalues have a positive real part, the steady-state regime is asymptotically stable. An eigenvalue lying in the right-hand half of the complex plane means that one of the following kinds of instability will occur in the circuit:

1) for $\omega = 0$, the amplitudes of the spectral lines of the steady-state regime, once perturbed, will grow exponentially in time;

2) for $\omega \neq 0$, an exponentially increasing power will be transferred from the steady-state regime to a spurious oscillation whose low-level fundamental frequency is ω.

In the first case, the equilibrium condition is intrinsically unstable. In the second case, the present analysis can only detect the onset of the spurious oscillation, but is unable to find its steady-state amplitude and frequency, because of its perturbation approach.

The stability analysis is considerably simplified by two important properties of the determinant Δ, to be discussed below. First, as a straightforward consequence of being $C_{m-p} = C_{mp}^*$, $D_{m-p} = D_{mp}^*$ (because the partial derivatives

in (11) are real) and $Y(\sigma + j\omega) = Y^*(\sigma - j\omega)$, we get

$$A_{k,s-k}(\sigma + j\omega) = A^*_{-k,-(s-k)}(\sigma - j\omega) \tag{18}$$

where * denotes the complex conjugate. From (18) follows

$$\Delta(\sigma + j\omega) = \Delta^*(\sigma - j\omega) \tag{19}$$

so that the eigenvalues occur in complex conjugate pairs, as could be expected.

As a second point, we will show that, *when the matrix is of infinite order*, Δ is a periodic function of ω.

In fact, by inspection of (14) we find that, for fixed p and k large and positive

$$A_{-k,p} \cong (-1)^n A_{k,p}. \tag{20}$$

Furthermore, if h is an integer, since C_{mp} and D_{mp} are independent of ω, (14) yields

$$A_{k,s-k}\{\sigma + j(\omega + h\omega_0)\} = A_{k+h,(s+h)-(k+h)}(\sigma + j\omega) \tag{21}$$

so that adding $h\omega_0$ to ω merely results in shifting the system matrix by h places in the direction of its principal diagonal. Due to (20), we thus have

$$\Delta\{\sigma + j(\omega + h\omega_0)\} = (-1)^{nh}\Delta(\sigma + j\omega). \tag{22}$$

In most practical cases, one is essentially interested in determining the stability of the steady-state regime rather than the solutions of (17). This can be accomplished by applying Nyquist's analysis to the determinant $\Delta(\sigma + j\omega)$ [8].

Since (14) is an integer function of the passive-network admittance, which is positive-real, Δ has no singularities for $\sigma > 0$ (except at infinity). On the imaginary axis, provided that losses in the passive circuit be taken into account, the determinant has a pole of order l at each of the points $\omega = k\omega_0$ $(-\infty < k < \infty)$, as clearly appears by inspection of (14). Thus, the Nyquist equation may be written in the form

$$N_T = N_Z - N_\infty + \tfrac{1}{2}N_{IZ} - \tfrac{1}{2}N_{IP} \tag{23}$$

where

- N_T number of clockwise encirclements of the origin made by $\Delta(j\omega)$ as ω is swept from $-\infty$ to $+\infty$;
- N_Z number of zeros of $\Delta(\sigma + j\omega)$ lying in the right-half complex plane;
- $-N_\infty$ contribution to N_T arising from the singular behavior of $\Delta(\sigma + j\omega)$ at infinity (i.e., as $(\sigma + j\omega) \to \infty$ with $\sigma > 0$);
- N_{IZ} number of zeros of the determinant lying on the imaginary axis;
- N_{IP} number of poles of the determinant lying on the imaginary axis.

In principle N_{IZ} could be found directly from the Nyquist plot of $\Delta(j\omega)$; however, the existence of such zeros is physically anomalous and numerically impossible, and will thus be disregarded ($N_{IZ} = 0$).

No matter what the values of N_Z and N_{IP}, because of (22), $\Delta(j\omega)$ makes n counterclockwise encirclements of the origin when ω is swept across any interval of length $2\omega_0$. Equation (23) shows that such encirclements derive from the singularity of Δ at infinity. Since the function

$$\exp\left\{\frac{n\pi}{\omega_0}(\sigma + j\omega)\right\} \tag{24}$$

exhibits exactly the same behavior, we may conclude that (24) and Δ have the same singularity as $(\sigma + j\omega) \to \infty (\sigma > 0)$.

Now, consider the function

$$\exp\left\{-\frac{n\pi}{\omega_0}(\sigma + j\omega)\right\}\cdot\Delta(\sigma + j\omega). \tag{25}$$

It is clear that (25) has the same zeros as $\Delta(\sigma + j\omega)$ but is finite for $(\sigma + j\omega) \to \infty (\sigma > 0)$, i.e., for it $N_\infty = 0$. Thus, it is convenient to use (25) instead of Δ alone in the Nyquist analysis. Furthermore, (25) is a periodic function of ω with period ω_0, so that only the range $[0, \omega_0]$ need be considered to obtain the complete Nyquist plot. This represents an essential feature in view of the practical implementation of the above theory, since a numerical evaluation of the behavior of $\Delta(j\omega)$ on the entire j axis would be impossible due to the complicated expression of the determinant. Because of this periodicity, (25) has a pole of order l in any interval of the j axis of length ω_0.

We may now write the Nyquist equation for (25) referring to the interval $[0, \omega_0]$ in the form

$$n_Z = n_T + \frac{l}{2} \tag{26}$$

where

- n_Z number of zeros of $\Delta(\sigma + j\omega)$ lying in the region $[0 \leqq \omega < \omega_0, \sigma > 0]$;
- n_T number of clockwise encirclements of the origin made by $\Delta(j\omega)$ as ω is swept from 0 to ω_0.

When $l = 0$, the Nyquist plot is closed and bounded. When $l > 0$, it is unbounded but includes l infinite semicircles (described in the clockwise sense) which close it at infinity [8]. Finally, because of (19), the plot is symmetric with respect to the real axis, so that one only has to study the range $[0, \omega_0/2]$ in order to complete the analysis.

For practical computation, the infinite problem (16) must be truncated to a finite dimension, i.e.,

$$\begin{cases} \sum_{k=-N}^{N} A_{k,s-k}\Delta V_k = 0 \\ -N \leqq s \leqq N. \end{cases} \tag{27}$$

When doing so, the integer N should be carefully chosen if physically and numerically accurate results are sought. The Fourier expansions of the derivatives (11) must be truncated, too, by retaining a finite number N_D of harmonics. Then (14) shows that, in order to approximately preserve the periodicity of (25) at least in the interval $[0, \omega_0]$, we must take

$$N - N_D \gg 1 \tag{28}$$

the degree of approximation being established by the actual value of the left-hand side of (28).

In some cases, such as circuits containing $p-n$ or Schottky junctions driven into forward conduction, the derivatives may be quite broadbanded because of the exponential functions appearing in the device equations. A number of harmonics of the order of 30 or more may be required for an accurate representation of the derivatives, which implies $N \geqq 50$ to obtain a 5-percent accuracy, according to (28). The numerical problem then becomes very large, since the size of the truncated system (27) is of the order of one hundred. In practice, such very stringent requirements may often be considerably released, as we will show in the next section. In any case, the cost-effectiveness of the solution can be dramatically improved by implementation of the method on a vector processor; in fact, the matrix formulation described above is ideally suited for taking advantage of the high computational power of a vector hardware, especially for large-size problems.

III. Examples of Application

A. Monochromatic Free-Running Oscillator Subject to Slowly Changing Perturbations

We consider a steady-state regime of the form

$$\tilde{i}(t) = \mathrm{Re}\left[\tilde{I}\exp(j\omega_0 t)\right]$$
$$\tilde{v}(t) = \mathrm{Re}\left[\tilde{V}\exp(j\omega_0 t)\right] \tag{29}$$

(all harmonics negligible) where $\tilde{V} = V\exp(j\phi_0)(V > 0)$. The stability analysis of (29) will be restricted to those perturbations that are *slowly changing* in time with respect to the fundamental, i.e., can be reduced to

$$\Delta i(t) = \exp(\sigma t)\cdot \mathrm{Re}\left[\Delta I \exp\{j(\omega+\omega_0)t\}\right]$$
$$\Delta v(t) = \exp(\sigma t)\cdot \mathrm{Re}\left[\Delta V \exp\{j(\omega+\omega_0)t\}\right] \tag{30}$$

where

$$|\sigma + j\omega| \ll \omega_0. \tag{31}$$

Due to (29) and (30), only the $s = k = 1$ term appears in the solving system (16), so that the eigenvalue equation (17) is reduced to

$$\Delta(\sigma + j\omega) = A_{10} = 0. \tag{32}$$

The nonlinear device can be described in terms of a "device admittance" when its time-domain equation has the general form

$$-\sum_{m=-l}^{n} a_m F^m i + F\left[F^{-l}v, \cdots, F^n v\right] = 0 \tag{33}$$

which is a particular case of (1). Just for the sake of clarity, in the following we will make use of the simplified expression:

$$-i(t) + F\left[v(t), \frac{dv}{dt}\right] = 0. \tag{34}$$

From (34) and (11), we obtain $C_{00} = -1$, $C_{mp} = 0$ (for m or $p \neq 0$), $D_{mp} = 0$ (for $m > 1$), so that (32) reduces to

$$A_{10} = D_{00} + \{\sigma + j(\omega+\omega_0)\}D_{10} + Y(\omega_0+\omega-j\sigma) = 0 \tag{35}$$

or, by the assumption of slowly changing perturbation

$$D_{00} + \{\sigma + j(\omega+\omega_0)\}D_{10} + Y(\omega_0) + \frac{dY}{d\omega}\cdot(\omega - j\sigma) = 0 \tag{36}$$

the derivative being evaluated at $\omega = \omega_0$.

We now introduce the quantity

$$Y_D(\omega, V) = \frac{\tilde{I}}{\tilde{V}} = \frac{1}{\pi V}\int_0^{2\pi} F[V\cos x, -\omega V \sin x]e^{-jx}\,dx \tag{37}$$

which is conventionally named "device admittance." From (37) and the expansions (11), we get

$$\frac{\partial}{\partial V}\{VY_D(\omega, V)\} = D_{00} + j\omega_0 D_{10} + \exp(-j2\phi_0)\cdot\{D_{02} - j\omega_0 D_{12}\}$$
$$\frac{\partial}{\partial \omega}Y_D(\omega, V) = jD_{10} - j\exp(-j2\phi_0)D_{12} \tag{38}$$

all derivatives being evaluated in steady-state conditions. Note that, for a slowly changing perturbation, D_{02} and D_{12} must be negligible, so that (38) can be reduced to

$$D_{10} \cong -j\frac{\partial Y_D}{\partial \omega}$$
$$D_{00} \cong Y_D(\omega_0, V) + V\frac{\partial Y_D}{\partial V} - \omega_0\frac{\partial Y_D}{\partial \omega}. \tag{39}$$

Finally, we define the admittance

$$Y_T(\omega, V) = G_T(\omega, V) + jB_T(\omega, V) = Y_D(\omega, V) + Y(\omega) \tag{40}$$

and remember the steady-state equilibrium condition $Y_T(\omega_0, V) = 0$, to obtain from (36)

$$(\omega - j\sigma)\frac{\partial Y_T}{\partial \omega} = -V\frac{\partial Y_T}{\partial V} \tag{41}$$

or

$$\sigma = \mathrm{Im}\left[V\frac{\frac{\partial Y_T}{\partial V}}{\frac{\partial Y_T}{\partial \omega}}\right] = V\frac{\frac{\partial B_T}{\partial V}\frac{\partial G_T}{\partial \omega} - \frac{\partial G_T}{\partial V}\frac{\partial B_T}{\partial \omega}}{\left|\frac{\partial Y_T}{\partial \omega}\right|^2}. \tag{42}$$

The stability condition $\sigma < 0$ then becomes

$$\frac{\partial G_T}{\partial V}\frac{\partial B_T}{\partial \omega} - \frac{\partial B_T}{\partial V}\frac{\partial G_T}{\partial \omega} > 0 \tag{43}$$

as was found by Hansson and Lundström [6] and previously by Kurokawa [5] (the latter for the case of a purely resistive nonlinear device).

B. Microstrip Parametric Frequency Divider

In this section, we apply the stability analysis to the nonlinear microstrip network whose topology is schematically illustrated in Fig. 2. This circuit was designed (in the

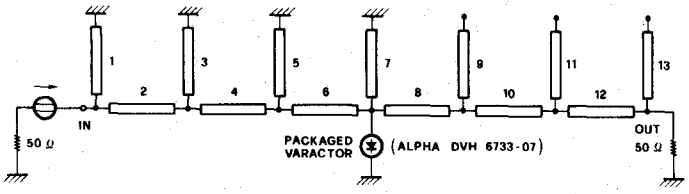

Fig. 2. Transmission-line model of microstrip frequency divider.

TABLE I
MICROSTRIP DIMENSIONS

n.	Width (mm)	Length (mm)	n.	Width (mm)	Length (mm)
1	8.9	25.4	8	1.1	13.1
2	8.4	18.4	9	6.1	20.7
3	6.6	34.1	10	5.1	22.5
4	6.8	23.6	11	4.6	14.3
5	8.1	19.9	12	3.2	20.6
6	7.7	22.0	13	1.3	24.4
7	8.9	14.0	SUBSTRATE: 1.58 mm DUROID		

way described in [9]) to act as a frequency divider by 2 in a 500-MHz band centered at 2.375 GHz (input frequency), with an insertion loss in the 4–6-dB range at a nominal input power level of 9 dBm. The divider geometry is given in Table I in terms of microstrip widths and lengths; all diode parameters including parasitics are available from the manufacturer's catalog (ALPHA Industries Silicon abrupt-junction varactor model DVH 6733-07).

For the present case, the nonlinear device is a microwave varactor represented in the time domain by [10]

$$-i + I_S\left[\exp\left(\frac{ev}{xK_BT}\right)-1\right] + \left[C_{T0}\left(1-\frac{v}{\phi}\right)^{-\gamma} + C_{D0}\exp\left(\frac{ev}{xK_BT}\right)\right]\frac{dv}{dt} = 0 \quad (44)$$

where

I_S saturation current,
e electron charge,
x slope (or ideality) factor of current,
K_B Boltzmann's constant,
T absolute temperature,
ϕ diffusion potential,
C_{T0} zero-bias depletion-layer (transition) capacitance,
C_{D0} zero-bias diffusion capacitance.

The varactor is unbiased and is thus drawn into forward conduction during a considerable fraction of the RF cycle. However, the calculations show that the forward voltage is always definitely less than the diffusion potential, so that no numerical ill-conditioning can occur in (44). Thus, (44) can be used to obtain explicit expressions for the derivatives; from (14), the coefficients are then found to be

$$A_{k,p} = D_{0p} + \{\sigma + j(\omega + k\omega_0)\}D_{1p} - \delta_p^0 Y(\omega - j\sigma + k\omega_0), \qquad \delta_p^0 = 1 \text{ for } p = 0, \quad 0 \text{ otherwise.} \quad (45)$$

Due to the exponentials appearing in (44), the derivatives usually have a considerably broader bandwidth than

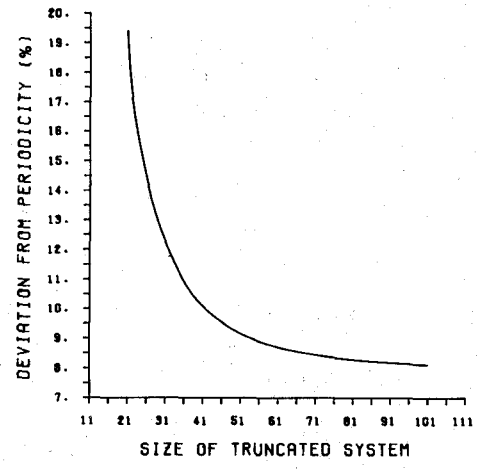

Fig. 3. Truncation error introduced when reducing the infinite solving system to a finite size.

the steady-state regime. For the present purposes, ten frequency components [9] were used in (4) to accurately describe the equilibrium voltage and current waveforms; in the same conditions, $N_D = 35$ harmonics were required to compute the derivatives with a comparable accuracy by the Fourier expansions (11) truncated at $p = \pm N_D$. Taking $N = 50$ in (27), which means a system of order 101, then should allow the Nyquist plots to be computed with a maximum error of about 7 percent (for $0 \leq \omega < \omega_0$), according to (28). This prediction can be checked from Fig. 3, where we plot the deviation from periodicity of (25) in the range $[0, \omega_0]$ against the size of the truncated system, $2N+1$. The deviation is defined as

$$D = 100\left|\frac{\Delta(j\omega_0)+\Delta(0)}{\Delta(0)}\right| \quad (46)$$

since, for the present case, $n = 1$ in (25). The figure shows that $D \cong 8.1$ percent for the size of 101, which is considered satisfactory for practical purposes.

In the following, we first discuss in some detail a large-size solution of the stability problem based on the choices $N_D = 35$, $N = 50$, and making use of 250 frequency points evenly spaced in the range $[0, \omega_0]$ to draw the Nyquist plots. This is mainly intended to show that our method can indeed produce solutions of high numerical accuracy (which may be required in some critical cases), and that such solutions may still be quite cheap when using a vectorized code on a supercomputer. We then briefly comment on the possible tradeoffs between numerical accuracy and computer time requirements, and on the impact of this on the physical accuracy of the solutions.

In view of the implementation of the numerical approach on a vector processor, we note the following.

1) The passive network admittance appearing in (14) can be computed in parallel (in the pipeline sense) at all frequencies $(\omega + k\omega_0)$ by existing vectorized programs for microwave circuit analysis [11]. In this way, the time required for admittance calculations is reduced by more than one order of magnitude with respect to conventional computational methods on scalar machines [11].

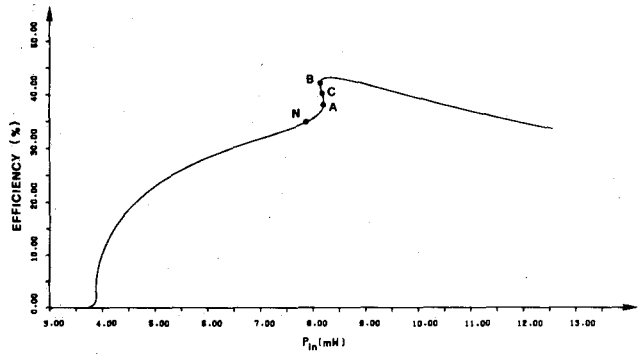

Fig. 4. Power transfer characteristic of parametric frequency divider.

2) Because of (14) and (27), the system matrix has a band structure with a total bandwidth $2N_D+1$. Thus, it can be computed and stored diagonal-wise with a unique vector operation. It is then rearranged column-wise (as required for determinant computation) making use of the gather-scatter capabilities of the vector processor.

3) Thanks to 1) and 2), the CPU time requirements are practically reduced to determinant computation only. The latter is clearly a highly vectorizable process which can be carried out most efficiently by existing mathematical routines (e.g., the vectorized library MAGEV on a Cyber 205).

As a result, a 250-point Nyquist plot can be found in about 16 s on a Cyber 205 (in the case $N_D=35$, $N=50$), as opposed to the 545's that are required to carry out the same calculations on a CDC 7600, with a speedup factor of 34. In this way, the numerical method becomes practically usable even for the most demanding applications.

Some results concerning the microstrip frequency divider of Fig. 1 are reported below. Fig. 4 is a plot of the power efficiency of the divider versus available input power at an input frequency of 2.5 GHz. To obtain this curve, the circuit of Fig. 1 was analyzed by the harmonic-balance technique at several input-power levels. In practice, the negative-slope section of the curve AB is replaced by a narrow hysteresis cycle, in much the same way as it is found in the different, but related, case of parametric multipliers [12]. This situation is closely matched by the results of the stability analysis. Fig. 5 gives the Nyquist plot for the nominal steady-state regime (point N in Fig. 4); the curve does not encircle the origin, denoting a stable spurious-free condition. On the other hand, the Nyquist plot for a point in the negative-slope region (point C in Fig. 4) is shown in Fig. 6; in this case, we have one clockwise encirclement, denoting the existence of one positive real eigenvalue. The corresponding equilibrium regime is thus intrinsically unstable and cannot exist in practice.

The curves in Figs. 5 and 6 were computed over the full range $[0, \omega_0]$. According to the theory developed in Section II, the first half of each Nyquist plot ($0 \leqq \omega \leqq \omega_0/2$), which is represented by a solid line in the figures, should be the exact mirror image (with respect to the real axis) of the remaining half, drawn by a dotted line. This condition is very closely met by the diagrams of Figs. 5 and 6, which

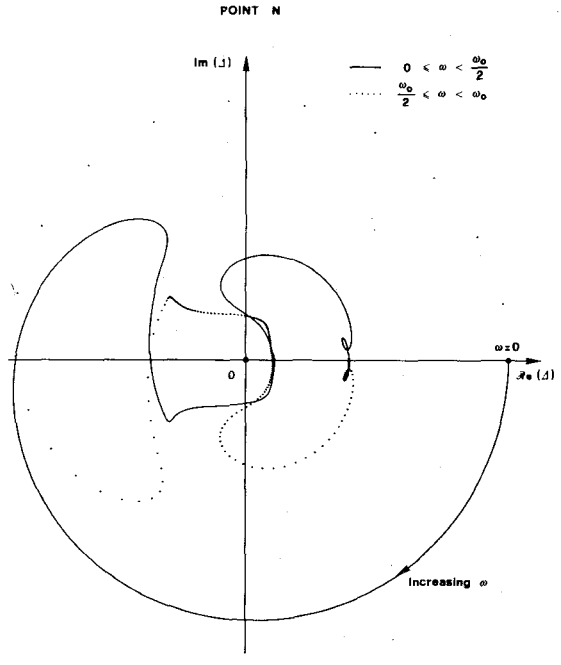

Fig. 5. Nyquist plot for a stable equilibrium condition of the frequency divider (nominal operating regime).

provides a clear check of the excellent accuracy of our results.

The information presented so far clearly shows that the computer time required to carry out a stability analysis can be considerably reduced (with respect to the high-accuracy solution discussed above) with no dramatic impairment of the final results. First of all, it is quite obvious that the calculations can actually be restricted to the range $[0, \omega_0/2]$ in routine applications, thus dividing by 2 the analysis cost. Furthermore, Fig. 3 suggests that the size of the truncated system can be reduced to some extent without a substantial degradation of the Nyquist plot, since the periodicity error actually drops more rapidly than one would predict, based on (28). For instance, a system of size 41 ($N=N_D=20$) yields a deviation from periodicity of about 10 percent in the present case, which is still acceptable for practical purposes. Finally, the number of frequency points used to build the Nyquist plot can also be decreased, as can be inferred from Figs. 5 and 6, provided that care be taken in order not to loose control on the plot behavior around the origin. In summary, it was found that a satisfactory stability analysis of the parametric divider can be carried out on a Cyber 205 in less than 1s, which is well below the time required for a typical nonlinear design. Thus, the idea of complementing existing general-purpose nonlinear CAD packages (e.g., [7]) by an on-line facility for automatic stability analysis becomes quite attractive.

A reduction of the number of harmonics to be dealt with in the analysis also tends to waive the need for an accurate description of both the nonlinear devices and the passive network at extremely high microwave frequencies. As an example, in the parametric divider case discussed so far, carrying out the stability analysis with $N=20$ means that the highest frequency of interest is about 25 GHz, which is

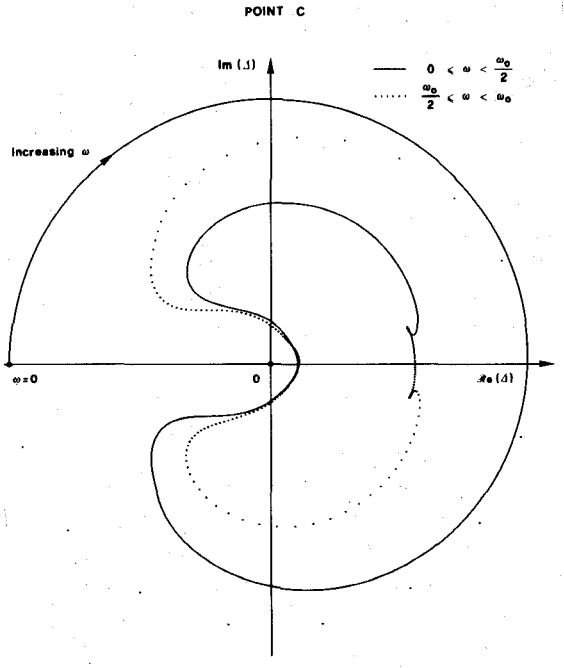

Fig. 6. Nyquist plot for an intrinsically unstable equilibrium condition of the frequency divider (hysteresis region).

well within the reach of present-day modeling capabilities. A substantially similar situation can be expected to occur in the case of a higher fundamental frequency, since then the number of significant harmonics of the steady-state regime becomes smaller, which in turn limits the number of spectral lines of the perturbation that must be accounted for. Generally speaking, the ability to keep track of any number of harmonics which is typical of the present computer approach should allow the designer to find the best compromise between physical and numerical accuracy in each particular case.

Acknowledgment

The authors are indebted to Control Data Italy, to Control Data France, and to the computing center CINECA (Casalecchio di Reno, Bologna, Italy) for providing access to the Cybernet Cyber 205 vector processor and for technical assistance during the preparation of the computer program described herein.

References

[1] C. A. Brackett, "Characterization of second-harmonic effects in IMPATT diodes," *Bell Syst. Tech. J.*, vol. 49, pp. 1777–1810, Oct. 1970.

[2] M. E. Hines, "Large-signal noise, frequency conversion and parametric instabilities in IMPATT diode networks," *Proc. IEEE*, vol. 60, pp. 1534–1548, Dec. 1972.

[3] J. Gonda and W. E. Schroeder, "IMPATT diode circuit design for parametric stability," *IEEE Trans. Microwave Theory Tech.*, vol. MTT-25, pp. 343–352, May 1977.

[4] E. F. Calandra and A. M. Sommariva, "Stability analysis of injection-locked oscillators in their fundamental mode of operation," *IEEE Trans. Microwave Theory Tech.*, vol. MTT-29, pp. 1137–1144, Nov. 1981.

[5] G. H. B. Hansson and K. I. Lundström, "Stability criteria for phase-locked oscillators," *IEEE Trans. Microwave Theory Tech.*, vol. MTT-20, pp. 641–645, Oct. 1972.

[6] K. Kurokawa, "Some basic characteristics of broadband negative resistance oscillator circuits," *Bell Syst. Tech. J.*, vol. 48, pp. 1937–1955, 1969.

[7] V. Rizzoli, A. Lipparini, and E. Marazzi, "A general-purpose program for nonlinear microwave circuit design," *IEEE Trans. Microwave Theory Tech.*, vol. MTT-31, pp. 762–770, Sept. 1983.

[8] J. J. Di Stefano, A. R. Stubberud, and I. J. Williams, *Feedback and Control Systems*. Los Angeles: McGraw-Hill: 1967, ch. 11.

[9] A. Lipparini, E. Marazzi, and V. Rizzoli, "A new approach to the computer-aided design of nonlinear networks and its application to microwave parametric frequency dividers," *IEEE Trans. Microwave Theory Tech.*, vol. MTT-30, pp. 1050–1058, July 1982.

[10] H. A. Watson, Ed., *Microwave Semiconductor Devices and Their Circuit Applications*. New York: McGraw-Hill, 1969.

[11] V. Rizzoli and M. Ferlito, "Vector processing concepts in microwave circuit design," in *Proc. 14th European Microwave Conf.* (Liège), Sept. 1984, pp. 847–852.

[12] E. Bava *et al.*, "Analysis of varactor frequency multipliers: Nonlinear behavior and hysteresis phenomena," *IEEE Trans. Microwave Theory Tech.*, vol. MTT-27, pp. 141–147, Feb. 1979.

Vittorio Rizzoli (M'79) was born in Bologna, Italy, in 1949. He graduated from the School of Engineering, University of Bologna, Bologna, Italy, in July 1971.

From 1971 to 1973, he was with the Centro Onde Millimetriche of Fondazione Ugo Bordoni, Pontecchio Marconi, Italy, where he was involved in a research project on millimeter-waveguide communication systems. In 1973, he was with the Hewlett–Packard Company, Palo Alto, CA, working in the areas of MIC and microwave power devices. From 1974 to 1979, he was an Associate Professor at the University of Bologna, teaching a course on microwave integrated circuits. In 1980, he joined the University of Bologna as a full Professor of Electromagnetic Fields and Circuits. His current fields of interest are the computer-aided analysis and design of nonlinear microwave circuits and the theoretical aspects of electromagnetic propagation in optical fibers.

Mr. Rizzoli is a member of AEI.

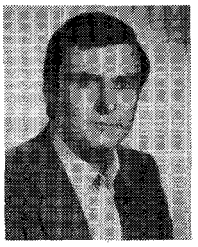

Alessandro Lipparini was born in Bologna, Italy, on August 31, 1947. He graduated with a degree in electronic engineering from the University of Bologna, Bologna, Italy, in 1974.

In 1974, he joined the Technical Staff of the Istituto di Elettronica, University of Bologna, as a Research Fellow. Since March 1975, he has been a Researcher for the Italian Ministry of Education at the University of Bologna, also serving as a Lecturer on Circuit Theory. Since 1983, he has been with the Department of Electronics, Computer Science and Systems Theory of the University of Bologna, where he is now teaching an Exercise Course on Electromagnetic Field Theory. His current research interests are in the fields of MIC and MMIC with special emphasis on nonlinear circuits. He is also involved in a research project aimed at the development of vectorized software for microwave circuit design applications.

Mr. Lipparini was awarded the G. Marconi Prize for Scientific Research in 1974, and is a member of AEI.